Available online at www.sciencedirect.com

ScienceDirect

Physics Procedia 64 (2015) 150 – 156

Physics Procedia

Scientific Workshop on Nuclear Fission dynamics and the Emission of Prompt Neutrons and Gamma Rays, THEORY-3

Neutron-induced fission measurements at the time-of-flight facility *n*ELBE

T. Kögler[a,b,*], R. Beyer[a], A. R. Junghans[a,**], R. Massarczyk[a,c], R. Schwengner[a], A. Wagner[a]

[a] *Helmholtz-Zentrum Dresden-Rossendorf, Postfach 510 119, 01314 Dresden, Germany*
[b] *Technische Universität Dresden, Postfach 100 920, 01076 Dresden, Germany*
[c] *Los Alamos National Laboratory, Los Alamos, New Mexico 87545, USA*

Abstract

Neutron-induced fission of ^{242}Pu is studied at the photoneutron source *n*ELBE. The relative fast neutron fission cross section was determined using actinide fission chambers in a time-of-flight experiment. A good agreement of present nuclear data with evaluations has been achieved in the range of 100 keV to 10 MeV.

Peer-review under responsibility of the European Commission, Joint Research Centre – Institute for Reference Materials and Measurements

Keywords: Neutron-induced fission, parallel plate fission ionization chambers, cross section measurements

1. Introduction

Recent sensitivity studies of future nuclear technologies [Working Party on International Evaluation Co-Operation (WPEC), 2008] show that a reduction of the total uncertainty of cross section data and core properties to below 7 % is needed to perform reliable simulations of nuclear reactors. Therefore cross section measurements, in particular of fast neutron induced fission, attracts growing interest.

Present neutron-induced fission cross section data on plutonium and minor actinides show large uncertainties in the neutron energy range from several tens of keV up to 10 MeV. Especially for ^{242}Pu the existing data sets differ by about 21 % [Otuka et al., 2014].

The present work describes an experiment studying the neutron-induced fission at the newly rebuilt compact neutron time-of-flight facility *n*ELBE. The facility covers the energy range of relevance for new types of fast reactors

* Corresponding author. Tel.: +49 351 265 3281
** Principal corresponding author.
E-mail address: t.koegler@hzdr.de, a.junghans@hzdr.de

Peer-review under responsibility of the European Commission, Joint Research Centre – Institute for Reference Materials and Measurements
doi:10.1016/j.phpro.2015.04.020

and transmutation devices [Beyer et al., 2013; Junghans et al., 2013]. Improved beam power and a low-scattering environment provide excellent experimental conditions to perform high-precision experiments.

2. Experimental Setup

For the determination of fission cross sections, fission ionization chambers are the devices of choice [Knoll, 2010]. With their high intrinsic efficiency ionization chambers are well suited to perform these kinds of experiments.

Two fission chambers (^{235}U and ^{242}Pu, details in [Kögler et al., 2013a,b]) have been developed at the Helmholtz-Zentrum Dresden-Rossendorf (HZDR). The included fission samples were produced at the Institute for Nuclear Chemistry of the University of Mainz by molecular plating [Vascon et al., 2015]. The homogeneity of these very thin actinide targets (^{235}U: $n_A \approx 450$ μg/cm^2, ^{242}Pu: $n_A \approx 150$ μg/cm^2) was improved by using titanium coated silicon wafer as backing material (cf. Fig. 1).

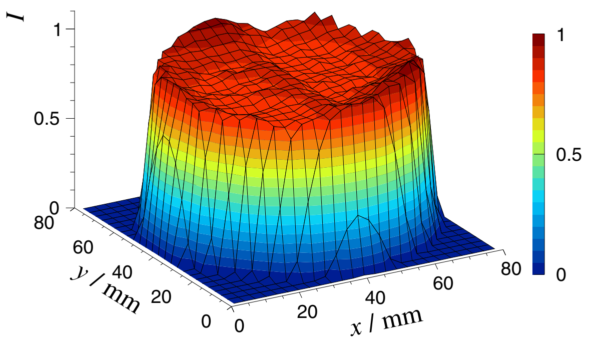

Fig. 1. Radiographic image of a ^{242}Pu target included in the fission chamber. The image (refer to [Vascon et al., 2015]) reflects the activity distribution of the sample, which is related to its homogeneity. A homogeneous target is important for the precise examination of neutron-induced fission cross sections, if an inhomogeneous neutron beam smaller than the target area is used.

To avoid uncertainties related to beam inhomogeneity, a sample diameter of 74 mm was chosen that is larger than the *n*ELBE beam diameter. Both fission chambers were mounted face-to-face within the neutron beam, whereby the uranium chamber was placed closer to the neutron source. The flight path of the neutrons was between 596.5 cm for the first uranium layer and 639.9 cm for the last plutonium layer. A sketch of the experimental setup is shown in Fig. 2.

Both fission chambers were operated in the forward biasing mode, which means that the fission targets are cathodes on positive potential. The anode was read out by a nanosecond preamplifier, which was developed at HZDR. Compared to conventional µs-shaping time preamplifiers, this device enables total signal lengths in the order of 200-400 ns. This reduces the α pile-up probability $P_n(R, \tau)$ drastically (95 % $\xrightarrow{\tau=5\,\mu\mathrm{s}\rightarrow 400\mathrm{ns}}$ 21 %). This probability [Knoll, 2010] is defined by:

$$P_n(R, \tau) = \frac{(R\tau)^n e^{R\tau}}{n!}, \tag{1}$$

where R denotes the expected detection rate and τ the time window, in which n particles additional to the primary one are detected by the same detector. For large detection rates R, higher order of piled-up events get important, because the produced signature in the detector could then be similar to a fission fragment [Kögler et al., 2013b].

The output signal of the preamplifier was splitted to measure its charge and the timing information. The latter determines the time of flight of the incident neutrons. A scheme of the VME based data acquisition electronics is shown in Fig. 3.

The time of flight was measured as the time difference between the accelerator RF pulse and the signal of the fission chamber. An MBS [Kurz and Essel, 2010] based data acquisition recorded list-mode data containing the QDC, TDC

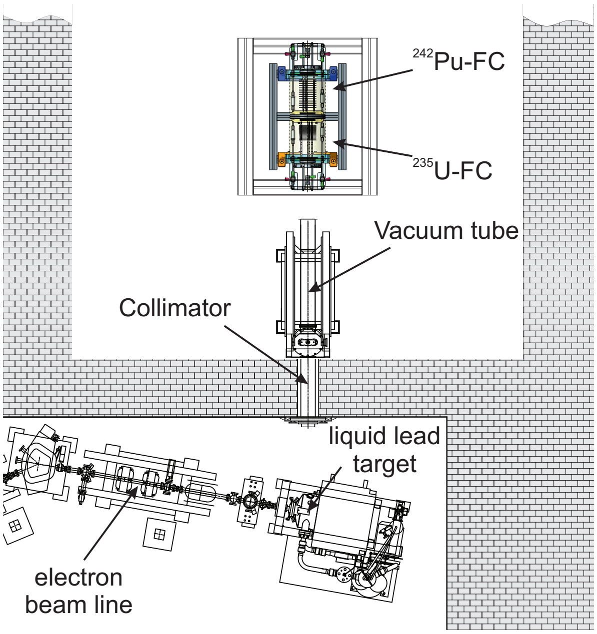

Fig. 2. Floor plan of *n*ELBE (not to scale). The ELBE electron beam is coming from the lower left side and hits the liquid lead circuit of the photoneutron source. Inside the liquid lead the electrons are decelerated and produce bremsstrahlung-photons, which in turn generate neutrons via (γ,n)-reactions on the lead nuclei. The neutrons are emitted isotropically and part of them enter to the low-scattering experimental area through a collimator. An evacuated beam tube is mounted inside the collimator and reaches 1 min the cave to avoid scattering on air. Traveling about 600 cm the neutrons reach the fission chambers.

and Scaler values of both detectors. Details of the setup and the related dead-time correction are given in Ref. [Beyer et al., 2013].

The experiment was carried out with an electron beam energy of 30 MeV, a repetition rate of 406.25 kHz and a mean bunch charge of approximated 73 pC.

3. Experimental results

The acquired time-of-flight spectra were calibrated with respect to the bremsstrahlung peak. The neutron time-of-flight was then calculated using:

$$t_n = f \cdot (ch_n - ch_\gamma) + \frac{L}{c}, \tag{2}$$

where $f = 0.9766$ ns/channel is the TDC dispersion, ch_n is the channel number in the time-of-flight spectrum, ch_γ is the channel number of the bremsstrahlung peak, L the flight path to the i^{th} fission target and c the speed of light.

Time-independent background from α-particles coming from the radioactive decay of the target nuclei was filtered out by applying a gate on the QDC values (cf. Fig. 4).

Fission events caused by room-returned background and spontaneous fission, which is crucial for ^{242}Pu, were subtracted by approximating a constant value in front of the bremsstrahlung peak, between this peak and the begin of the neutron-induced fission events and at the end of the spectrum (cf. Fig. 5).

After the background has been subtracted a translation from neutron time-of-flight to neutron kinetic energy was performed:

$$E_n = m_n c^2 \left(\frac{1}{\sqrt{1 - \left(\frac{L}{t_n c}\right)^2}} - 1 \right) \tag{3}$$

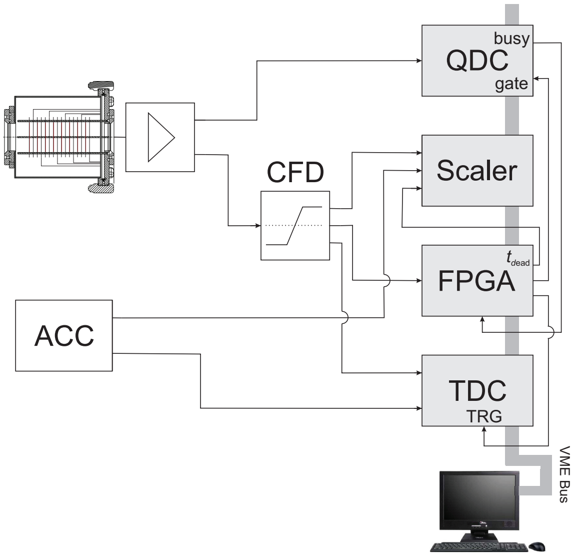

Fig. 3. Electronic scheme of the nELBE fission experiment. The scheme shows the data processing of one of 2x8 fission chamber channels. Each anode is connected to a charge-sensitive (nanosecond) preamplifier. The amplified signal is splitted and used to determine the charge- and timing information of the signal. The charge is measured by a CAEN V965A dual-range QDC. The second amplifier output signal feeds a fast constant-fraction discriminator (CFD) developed in-house to minimize the time walk over a large dynamic range required to detect all fission fragment signals. The output of the CFD are used to generate a trigger within a CAEN V1495 FPGA module (global "or" of all fission chamber channels), to measure the count-rate of the fission chamber channels (CAEN V1495, Scaler) and to determine the neutron time of flight relative to the accelerator (ACC) in a multi-event, multi-hit CAEN V1290N TDC. The experiments live and real time is determined also by the Scaler processing the busy signal of the QDC and the transfer time of the whole DAQ.

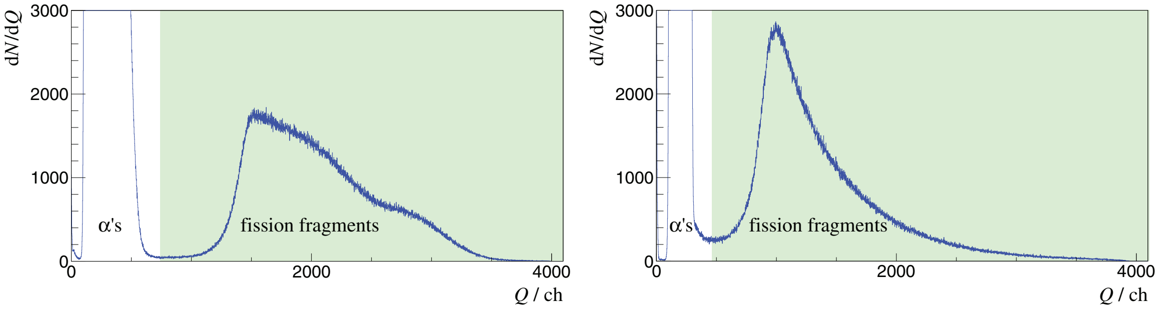

Fig. 4. Charge-spectra of one ^{242}Pu deposit (left) and one ^{235}U deposit (right). A good separation between α-particles and fission fragments is seen. This is an additional evidence of the very good quality of the fission targets. The shaded area marks the region of clearly identified fission fragments, which is used to suppress the constant background of the α-particles in the time-of-flight spectra.

The neutron-induced fission cross section was calculated using equation (4).

$$\sigma_f^{Pu}(E_n) = \underbrace{\frac{N_{in}^U}{N_{in}^{Pu}} \cdot \frac{n_A^U}{n_A^{Pu}}}_{k} \cdot \frac{\dot{N}_f^{Pu}}{\dot{N}_f^U} \cdot \sigma_f^U(E_n) = k \cdot \frac{\dot{N}_f^{Pu}}{\dot{N}_f^U} \cdot \sigma_f^U(E_n) \tag{4}$$

In this formula $\dot{N}_f$ stands for the live-time corrected count rates of fission events in an energy bin of the time-of-flight spectrum of the uranium or the plutonium chamber, N_{in} is the number of incident neutrons and n_A denotes the areal mass-density of the fission layer. Choosing two neighboring fission samples of the uranium and plutonium

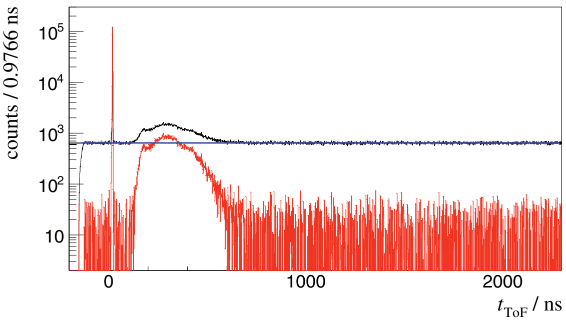

Fig. 5. Time-of-flight spectra of one channel of the ^{242}Pu (left) and the ^{235}U (right) fission chamber. The black histograms show distributions including the total number of acquired fission events. A time-independent background was determined by adjusting a constant value over the three regions mentioned in the text. This adjustment was extended over the whole range and is drawn as a blue line. The red histograms show the total spectra after subtraction of this constant background.

chamber, the neutron scattering correction on other material in the beam except the two steel windows of the chambers could be neglected. Together with the ratio of the areal-density of both actinide layers this can be condensed in a constant k. The constant k is adjusted to fit the existing data. The outcome of this adjustment is shown in Fig. 6.

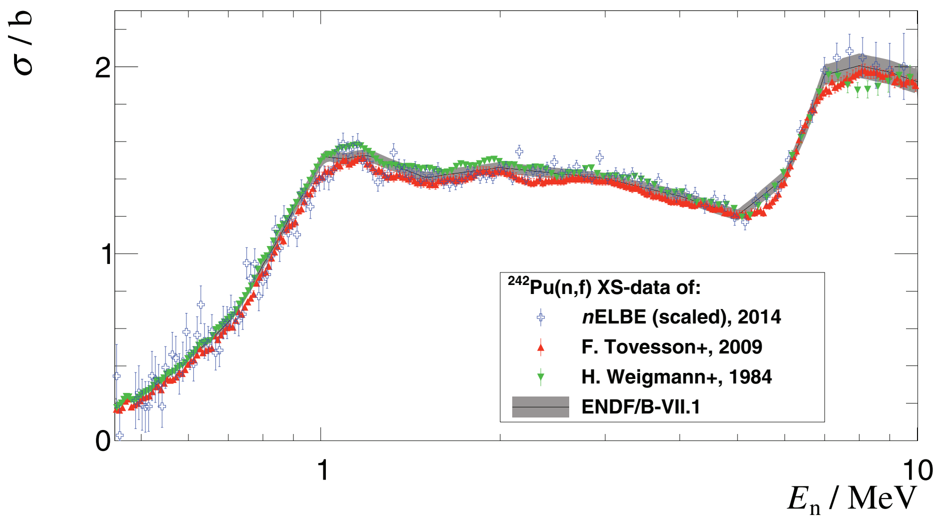

Fig. 6. Neutron-induced fission cross section of ^{242}Pu determined at *n*ELBE (blue data points). The data is shown together with two selected data sets from Tovesson et al. (red) and Weigmann et al. (green). The evaluated nuclear data from the ENDF/B-VII.1 database [Chadwick et al., 2011] is shown with a solid black line together with its gray shaded uncertainty band. The *n*ELBE data is in good agreement with the reference data, even though only data of one fission chamber channel is shown. Since the areal density of the fission target has not been determined so far, the data has been scaled to the evaluated data.

Presented here is only the data of one fission target of the plutonium chamber relative to one uranium target. Combining data of all acquired channels requires a scattering correction with neutron transport codes such as MCNP 5 [X-5 Monte Carlo Team, 2005] and Geant 4 [Allison et al., 2003]. Simulations of that kind are in progress. The current data was adjusted to the evaluated data set by fitting of k, because an absolute normalization has not been performed so far. Various measurements to determine the number of fissionable nuclei have already been performed at *n*ELBE and PTB Braunschweig. The analysis of this data is ongoing.

4. Conclusions

Two parallel plate fission ionization chambers have been developed, constructed and tested successfully. The excellent quality of the actinide layers was proven using radiographic images and the *n*ELBE neutron beam. The separation between α-induced background events and fission fragments is very good. The neutron-induced fission cross section of ^{242}Pu was determined in one week of *n*ELBE beam time relative to the uranium chamber. Preliminary data with only part of the statistics show a good agreement to present evaluated and measured data, in spite of the fact that the number of fissionable nuclei has not been determined. Measurements in the open neutron field of PTB Braunschweig, relative to the well characterized ^{235}U transfer device H19 [Gayther, 1990; Nolte et al., 2007] and of the spontaneous fission rate of ^{242}Pu have been performed to determine this number. The analysis of these experiments is in progress.

Acknowledgements

We would like to thank Manfred Sobiella and Klaus Heidel for the support in the construction of the fission chamber and the preamplifiers. We also thank Andreas Hartmann for the continuous support in the preparation of our experiments. Special thanks go to Alessio Vascon and Klaus Eberhardt from the Johannes Gutenberg University of Mainz for their effort in the production of our target samples. Thanks also go to the ELBE accelerator crew and all of the colleagues, who have participated during the experiments. This work was supported by the German Federal Ministry of Education and Research under contract no. 02NUK13A.

References

Allison, J., Agostinelli, S., Amako, K., Apostolakis, J., Araujo, H., Arce, P., Asai, M., Axen, D., Banerjee, S., Barrand, G., Behner, F., Bellagamba, L., Boudreau, J., Broglia, L., Brunengo, A., Burkhardt, H., Chauvie, S., Chuma, J., Chytracek, R., Cooperman, G., Cosmo, G., Degtyarenko, P., Dell'Acqua, A., Depaola, G., Dietrich, D., Enami, R., Feliciello, A., Ferguson, C., Fesefeldt, H., Folger, G., Foppiano, F., Forti, A., Garelli, S., Giani, S., Giannitrapani, R., Gibin, D., Cadenas, J. G., González, I., Abril, G. G., Greeniaus, G., Greiner, W., Grichine, V., Grossheim, A., Guatelli, S., Gumplinger, P., Hamatsu, R., Hashimoto, K., Hasui, H., Heikkinen, A., Howard, A., Ivanchenko, V., Johnson, A., Jones, F., Kallenbach, J., Kanaya, N., Kawabata, M., Kawabata, Y., Kawaguti, M., Kelner, S., Kent, P., Kimura, A., Kodama, T., Kokoulin, R., Kossov, M., Kurashige, H., Lamanna, E., Lampén, T., Lara, V., Lefebure, V., Lei, F., Liendl, M., Lockman, W., Longo, F., Magni, S., Maire, M., Medernach, E., Minamimoto, K., de Freitas, P. M., Morita, Y., Murakami, K., Nagamatu, M., Nartallo, R., Nieminen, P., Nishimura, T., Ohtsubo, K., Okamura, M., O'Neale, S., Oohata, Y., Paech, K., Perl, J., Pfeiffer, A., Pia, M., Ranjard, F., Rybin, A., Sadilov, S., Salvo, E. D., Santin, G., Sasaki, T., Savvas, N., Sawada, Y., Scherer, S., Sei, S., Sirotenko, V., Smith, D., Starkov, N., Stoecker, H., Sulkimo, J., Takahata, M., Tanaka, S., Tcherniaev, E., Tehrani, E. S., Tropeano, M., Truscott, P., Uno, H., Urban, L., Urban, P., Verderi, M., Walkden, A., Wander, W., Weber, H., Wellisch, J., Wenaus, T., Williams, D., Wright, D., Yamada, T., Yoshida, H., Zschiesche", D., 2003. Geant4 – a simulation toolkit. Nucl. Instr. and Meth. A 506 (3), 250 – 303.
URL `http://www.sciencedirect.com/science/article/pii/S0168900203013688`

Beyer, R., Birgersson, E., Elekes, Z., Ferrari, A., Grosse, E., Hannaske, R., Junghans, A., Kögler, T., Massarczyk, R., Matić, A., Nolte, R., Schwengner, R., Wagner, A., 2013. Characterization of the neutron beam at nELBE. Nucl. Instr. and Meth. A 723, 151 – 162.
URL `http://www.sciencedirect.com/science/article/pii/S0168900213005354`

Chadwick, M., Herman, M., Oblozinský, P., Dunn, M., Danon, Y., Kahler, A., Smith, D., Pritychenko, B., Arbanas, G., Arcilla, R., Brewer, R., Brown, D., Capote, R., Carlson, A., Cho, Y., Derrien, H., Guber, K., Hale, G., Hoblit, S., Holloway, S., Johnson, T., Kawano, T., Kiedrowski, B., Kim, H., Kunieda, S., Larson, N., Leal, L., Lestone, J., Little, R., McCutchan, E., MacFarlane, R., MacInnes, M., Mattoon, C., McKnight, R., Mughabghab, S., Nobre, G., Palmiotti, G., Palumbo, A., Pigni, M., Pronyaev, V., Sayer, R., Sonzogni, A., Summers, N., Talou, P., Thompson, I., Trkov, A., Vogt, R., van der Marck, S., Wallner, A., White, M., Wiarda, D., Young, P., 2011. ENDF/B-VII.1 Nuclear Data for Science and Technology: Cross Sections, Covariances, Fission Product Yields and Decay Data. Nucl. Data Sheets 112 (12), 2887 – 2996, special Issue on ENDF/B-VII.1 Library.
URL `http://www.sciencedirect.com/science/article/pii/S009037521100113X`

Gayther, D. B., 1990. International Intercomparison of Fast Neutron Fluence-Rate Measurements Using Fission Chamber Transfer Instruments. Metrologia 27 (4), 221.
URL `http://stacks.iop.org/0026-1394/27/i=4/a=006`

Junghans, A. R., Beyer, R., Grosse, E., Hannaske, R., Kögler, T., Massarczyk, R., Schwengner, R., Wagner, A., October 2013. Transmutation of high-level radioactive waste - Perspectives. Proceedings of the ERINDA workshop 2014-002.
URL `https://indico.cern.ch/event/251800/material/1/0.pdf`

Kögler, T., Beyer, R., Hannaske, R., Junghans, A., Massarczyk, R., Wagner, A., 2013a. Fission Experiments at nELBE. Physics Procedia 47, 178 – 183, Scientific Workshop on Nuclear Fission Dynamics and the Emission of Prompt Neutrons and Gamma Rays, Biarritz, France, 28-30

November 2012.
URL http://www.sciencedirect.com/science/article/pii/S1875389213004550

Kögler, T., Beyer, R., Hannaske, R., Junghans, A. R., Massarczyk, R., Schwengner, R., Wagner, A., October 2013b. The *n*ELBE (n,fis) experiment. Proceedings of the ERINDA workshop 2014-002.
URL https://indico.cern.ch/event/251800/material/1/0.pdf

Knoll, G. F., 2010. Radiation Detection and Measurement, 4th Edition. Wiley.

Kurz, N., Essel, H., May 2010. GSI Data Acquisition System MBS Release Notes V5.1. GSI, Gesellschaft für Schwerionenforschung mbH, Planckstraße 1, D-64291 Darmstadt, Germany, 5th Edition.
URL https://www.gsi.de/fileadmin/EE/MBS/2010_gm_mbs_rel_51.pdf

Nolte, R., Allie, M. S., Brooks, F. D., Buffler, A., Dangendorf, V., Meulders, J. P., Schuhmacher, H., Smit, F. D., Weierganz, M., 2007. Cross sections for neutron-induced fission of u-235, u-238, bi-209, and pb-nat in the energy range from 33 to 200 mev measured relative to n-p scattering. Nucl. Sci. Eng. 156 (2), 197–210.
URL http://www.new.ans.org/store/j_2696

Otuka, N., Dupont, E., Semkova, V., Pritychenko, B., Blokhin, A., Aikawa, M., Babykina, S., Bossant, M., Chen, G., Dunaeva, S., Forrest, R., Fukahori, T., Furutachi, N., Ganesan, S., Ge, Z., Gritzay, O., Herman, M., Hlavac, S., Kato, K., Lalremruata, B., Lee, Y., Makinaga, A., Matsumoto, K., Mikhaylyukova, M., Pikulina, G., Pronyaev, V., Saxena, A., Schwerer, O., Simakov, S., Soppera, N., Suzuki, R., Takács, S., Tao, X., Taova, S., Tárkányi, F., Varlamov, V., Wang, J., Yang, S., Zerkin, V., Zhuang, Y., 2014. Towards a More Complete and Accurate Experimental Nuclear Reaction Data Library (EXFOR): International Collaboration Between Nuclear Reaction Data Centres (NRDC). Nuclear Data Sheets 120 (0), 272 – 276.
URL http://www.sciencedirect.com/science/article/pii/S0090375214005171

Vascon, A., Runke, J., Trautmann, N., Cremer, B., Eberhardt, K., Düllmann, C., 2015. Quantitative molecular plating of large-area ^{242}Pu targets with improved layer properties. Applied Radiation and Isotopes 95, 36 – 43.
URL http://www.sciencedirect.com/science/article/pii/S0969804314003467

Working Party on International Evaluation Co-Operation (WPEC), 2008. Uncertainty and Target Accuracy Assessment for Innovative Systems Using Recent Covariance Data Evaluations. Tech. rep., OECD / NEA.
URL http://www.oecd-nea.org/science/wpec/volume26/volume26.pdf

X-5 Monte Carlo Team, 2005. MCNP — A General Monte Carlo N-Particle Transport Code, Version 5. Los Alamos National Laboratory, la-ur-03-1987 Edition.
URL https://laws.lanl.gov/vhosts/mcnp.lanl.gov/references.shtml#mcnp5_refs